

TENSION IN FLUTTERING FLAGS

Peter M. Moretti, Member IIAV

*Oklahoma State University, School of Mechanical & Aerospace Engineering,
Stillwater, OK 74078-5016, USA*

<http://www.mae.okstate.edu/Faculty/moretti/moretti.html>

When a flag flutters, tension is dynamically induced by the two-dimensional vibratory motion. The dynamic process, involving centrifugal forces due to the curved path of the trailing edge, is similar to the whipping of an oscillating rope, and accounts for most of the drag-force observed at the flagpole attachment (luff). Conversely, the induced tension, combined with the curvature of the fabric, opposes the pressure forces from the flow field and extracts momentum from it. In order to estimate post-critical flag and panel flutter amplitudes, it is necessary to compute the structural stiffening due to dynamically induced tension.

Tension in typical flag flutter motion, consisting of a traveling wave growing in amplitude as it progresses towards the trailing edge (leech), is obtained by approximate analysis, using a Computer Algebra System. The time-averaged tension depends on the square of the velocity amplitude of the oscillating fabric; the distribution of time-averaged tension is shown for a typical flag flutter motion. An estimate of the tension fluctuations is developed: the fluctuations are small (relative to the average tension) at locations several wavelengths from the leech, but are important near the leech.

The general P.D.E. of motion is obtained from Hamilton's principle. The induced-tension term in the governing P.D.E. derives from the in-plane kinetic energy of the flag motion. Dynamically induced tension is shown to be important if the stiffness of the fabric is low: an order-of-magnitude criterion is presented.

1 Introduction

Flag flutter is a challenging problem in physics. The stability limit is very low—flags can be observed to flutter even at very low wind speeds—and yet the flutter amplitudes and modes are steady. The prediction of flag-flutter

amplitudes could be a fundamental contribution to fluid/structure interaction. An accurate solution is difficult, and probably impossible without considering the dynamically induced tension terms derived below.

The three fundamental questions raised by flag flutter are:

1. Why does the flag flutter?
2. Why is the drag of a fluttering flag greater than that of a rigid vane?
3. What limits the amplitudes of a fluttering flag?

The first question was answered qualitatively by Thoma [1] when he pointed out that flow over a wavy surfaces produces an elevated pressure in the troughs and a reduced pressure over the crests, tending to increase the amplitudes. Sparenberg [2] confirmed that a traveling wave is generated.

The second question was raised by Fairthorne [3]. He observed that the increased drag varies directly with the mass-per-unit-area of the material, consistent with causation by the dynamics of the motion. Thoma [4] obtained the average tension in a waving rope, and linked it to the third question by pointing out that this dynamically induced tension tends to oppose the fluid-dynamic instability [1]. Our objective is to study the balance of forces.

When the flag curves, any tension tends to flatten the flag, opposing pressure differences across the flag. These pressure differences are complementary to the flow field around the flag. Conversely, the flow field around the flag generates pressure forces normal to the flag, accelerating the fabric; the resulting motions of the flag generate centrifugal forces which induce tension in the flag; and this tension opposes and ultimately limits the amplitudes of the flag motion.

This process dynamically transform normal (lift) forces on a flexible fabric into tension (drag) forces. It can be studied or measured either from the structural and from the fluid side:

- from the structural side, we can analyze the dynamics of the flag (as we will do below), or measure the drag forces at the flagpole; and
- from the fluid side, we can analyze the flow field, or measure the velocity profile in the wake.

The drag force must, of course, balance the momentum defect in the wake.

For the purpose of the initial physical analysis, the following simplifications will be made:

- A: The flag is perfectly *flexible*: the bending stiffness term is neglected.
- B: The flag is *inextensible*: the path length from luff to leech is constant.
- C: Gravity is neglected, and the deflections are uniform across the width.
- D: The flag is *wide* compared to wave-length: the flow-field is two-dimensional.
- E: Except for skin-friction calculations, the flow-field is potential flow.

The limitations introduced by these assumptions can be re-examined later.

2 Initial Stability

It has been proposed that flag flutter is caused either by vortex-shedding from the flagpole, or else by pressure-feedback from the vortex-street in the wake of a flat plate or sheet. However, observed flutter does not match either Strouhal frequency. Hence, our analysis looks for an instability phenomenon.

The governing equation of the flag for small deflections w as a function of time t and of distance x from the flagpole (luff) is

$$m_{flag} \frac{\partial^2 w}{\partial t^2} - T_{(x)} \frac{\partial^2 w}{\partial x^2} - \frac{\partial T}{\partial x} \frac{\partial w}{\partial x} + EI \frac{\partial^4 w}{\partial x^4} = \Delta p_{(t,x)} \quad (1)$$

where m_{flag} is the mass-per-unit-area of the flag, T is the tension-per-unit-width, and EI is the stiffness which we will neglect for now. Δp is the pressure difference generated by the flow field. In a paper on web spans [5] we have shown that the effect of a potential flow field can be replaced by aerodynamic mass terms resembling the “gyroscopic” inertia, Coriolis, and centrifugal coefficients of the Threadline Equation [6]

$$(m_{flag} + m_a) \frac{\partial^2 w}{\partial t^2} + 2m_a U_\infty \frac{\partial^2 w}{\partial t \partial x} + (m_a U_\infty^2 - T) \frac{\partial^2 w}{\partial x^2} - \frac{\partial T}{\partial x} \frac{\partial w}{\partial x} = 0 \quad (2)$$

where U_∞ is the far-field velocity of the surrounding air and m_a is the aerodynamically induced mass-per-unit-area. For very slender webs, $m_a = \pi \rho_{air} D^2/4$, a function only of web width D and air density ρ_{air} ; but for very wide webs with sinusoidal deflections of wavelength λ , it becomes $m_a = \rho_{air} \lambda/\pi$. While this aerodynamically-induced-mass representation is appropriate for continuous web spans, it is imperfect near the trailing edge (leech) of a flag, but still useful for approximate analysis.

Tension $T > m_a U_\infty^2$ is one necessary condition for the initial stability of a flexible flag. However, tension due to boundary-layer shear is small; at laminar Reynolds numbers, with viscosity μ , the normalized tension-per-unit-width is proportional to $\text{Re}^{-1/2}$, as summarized in Schlichting[7]

$$\frac{T_{drag}}{L\rho_{air}U_\infty^2} \cong 1.328\sqrt{\frac{(\mu_{air}/\rho_{air})}{U_\infty L}} \left[\frac{\sqrt{L} - \sqrt{x}}{\sqrt{L}} \right] \quad (3)$$

which peaks at the leading edge, but falls towards zero as we approach the trailing edge, $x \rightarrow L$, in Figure 1.

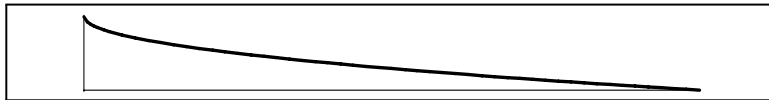


Figure 1: *Distribution of drag-induced tension T as a function of location x/L .*

At the leading (luff) edge, the tension is proportional to $U_\infty^{1.5}$ for laminar boundary layers (or to $U_\infty^{1.2}$ for turbulent boundary layers[8]). We see that a flag is unstable even at quite small U_∞ , at least near the trailing edge, unless we introduce some stiffness EI as in panel-flutter. Observations by Datta & Gottenberg [9] and Yamaguchi *et al.*[10] confirm that flexible flags begin to flutter at very low wind velocities.

3 Wave Form

Once flutter begins, additional tension is induced by the dynamic deflection w in the z -direction (normal to the initial plane of the flag). For the purpose of analysis, we postulate a deflection w which captures the essential features of the observed motion: a *traveling wave* within an envelope growing from a value of zero at the luff ($x = 0$) to the amplitude A at the leech ($x = L$), *e.g.*, in the form suggested by Thoma [1] and shown in Figure 2,

$$\begin{aligned} w &= \frac{A \sin(\alpha x/L)}{\sin(\alpha)} \cos(\omega t - \kappa x) \\ &= \frac{A}{2 \sin(\alpha)} \left[\sin\left(\omega t - \kappa x + \frac{\alpha}{L}x\right) - \sin\left(\omega t - \kappa x - \frac{\alpha}{L}x\right) \right] \end{aligned} \quad (4)$$

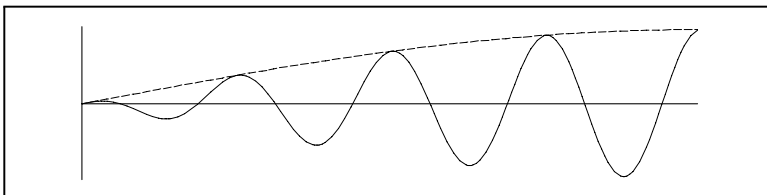


Figure 2: *Traveling wave within sinusoidal envelope.*

where the constant $\alpha \leq \pi/2$ is the shape parameter of the envelope. The simplest case, used by Uno [11], is to let $\alpha \rightarrow 0$, resulting in a *linearly increasing envelope* for the traveling wave shown in Figure 3.

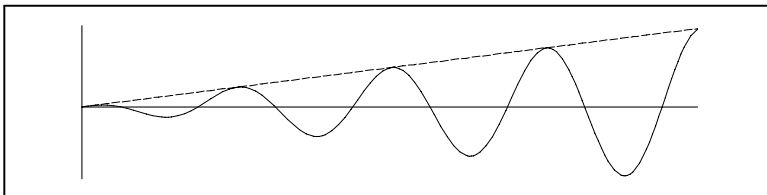


Figure 3: *Linearly growing traveling wave.*

$$w = \frac{Ax}{L} \cos(\omega t - \kappa x) \quad (5)$$

where A is the maximum amplitude; x is the distance along the flag measured from the luff; L is the maximum value of x ; and the frequency of the waves is $f = \omega/2\pi$. In this first approximation, κ is taken to be a constant; therefore, the *wave-length is assumed constant* at $\lambda = 2\pi/\kappa$ and phase velocity $c = f\lambda = \omega/\kappa$ is also constant.

Experimental observations by Watanabe *et al.*[12] on flutter of sheets and of slack edges of webs in paper machines, indicate that this description is appropriate over a wide range of air velocities. At very low velocities both Uno [11] and Watanabe *et al.*[12] observed similar behavior, but with a smaller number of waves within the length of the flag. At very high velocities, Taneda [13] observed an additional flapping motion at a higher frequency near the trailing edge, overlaid onto the basic flutter motion. In the presence of some amount of bending stiffness EI , both Taneda [13] and Watanabe

et al.[12] observed partial nodes, indicating some standing waves due to a certain amount of wave reflection at the trailing edge.

Similar wave forms have also been observed by Zhang *et al.*[14] on filaments in flowing soap films, which have been numerically simulated by Farnell, David, & Barton [15].

4 Time-average Tension

Thoma [4] analyzed the dynamically induced tension in an oscillating rope subjected to arbitrary normal forces (or a waving flag subjected to pressures). Writing V for velocity and T for tension, he derived a simple relationship for *time-averaged* tension as a function of distance s along the flag.

$$\frac{d\bar{T}}{ds} = -\frac{m_{flag}}{2} \cdot \frac{d}{ds} (\bar{V}^2) \quad (6)$$

Integrating along the length L of the flag, with uniform mass-per-unit-length m_{flag} from luff ($s = 0$) to leech ($s = L$), the average value of the tension at the attachment is

$$\bar{T}_{luff} = \frac{1}{2} m_{flag} \bar{V}^2_{leech} \quad (7)$$

Inserting our simple wave form and evaluating it near the tip ($x \cong L$)

$$\bar{V}^2_{leech} \cong \frac{A^2 \omega^2}{2} \quad (8)$$

we obtain the total dynamically-induced drag at the flagpole

$$\bar{T}_{luff} \cong \frac{m_{flag}}{2} \cdot \frac{A^2 \omega^2}{2} \quad (9)$$

Starting with Fairthorne [3], practical observations indicate that this is generally substantially greater than skin-friction drag.

Similarly, we can obtain the *time-averaged tension distribution* as a function of x

$$\begin{aligned} \bar{T}_{(x)} &= \frac{m_{flag}}{2} \cdot (\bar{V}^2_{leech} - \bar{V}^2_{(x)}) \\ &\cong \left(\frac{m_{flag}}{2} \cdot \frac{A^2 \omega^2}{2} \right) \left(1 - \frac{x^2}{L^2} \right) \end{aligned} \quad (10)$$

showing that the dynamically induced tension, shown in Figure 4, is distributed much more broadly than drag-induced tension.

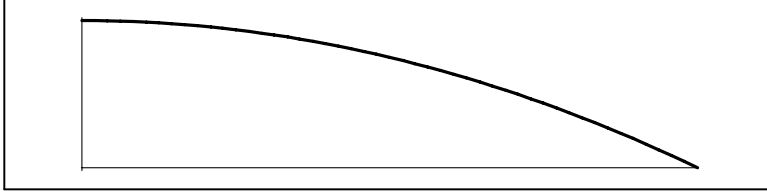


Figure 4: *Distribution of dynamically induced tension T as a function of location x/L .*

5 Tension Fluctuations

Using *Scientific WorkPlace* [16], which uses *Maple* as a Computer Algebra System, we begin by relating the path length s of the wave to coordinate x

$$\frac{ds}{dx} = \sqrt{1 + \left(\frac{dw}{dx}\right)^2} \quad (11)$$

The u -deflection in the (negative) x -direction (parallel to the free-stream velocity) is $u = x - s$. The position of an element of the flag is described by the w -deflection normal to the reference plane, plus the u -deflection in the reference plane of the flag. For moderate deflections and slopes, $(dw/dx)^2 \ll 1$, we can approximate the path length expression with the first two terms of the binomial expansion

$$\frac{ds}{dx} \cong 1 + \frac{1}{2} \left\{ \frac{A}{L} [\cos(\omega t - \kappa x) + x\kappa \sin(\omega t - \kappa x)] \right\}^2 \quad (12)$$

which simplifies the algebra considerably. We integrate, expand the terms to separate time and space variables, and obtain the longitudinal deflection and acceleration. Combining this with the transverse acceleration to obtain the acceleration vector, and relating it to the direction cosines of the flag itself, the change in tension with location is described by

$$\frac{dT}{dx} \cong - \left(\frac{A}{L}\right)^2 m_{flag} \frac{\omega^2}{\kappa} \left\{ \begin{array}{l} \frac{1}{2}\kappa x + \frac{1}{2} \cos \kappa x \sin \kappa x \\ - [\cos \kappa x \sin \kappa x] \cos^2 \omega t \\ - [\sin^2 \kappa x] \cos \omega t \sin \omega t \end{array} \right\} \quad (13)$$

which we can integrate to obtain tension

$$T \cong \left(\frac{A}{L}\right)^2 m_{flag} \frac{\omega^2}{\kappa^2} \left\{ \begin{array}{l} \frac{1}{4}(\kappa L)^2 - \frac{1}{4}(\kappa x)^2 \\ + [\frac{1}{8} \cos 2\kappa L - \frac{1}{8} \cos 2\kappa x] \cos 2\omega t \\ + [\frac{1}{8} \sin 2\kappa L - \frac{1}{8} \sin 2\kappa x - \frac{1}{4}\kappa L + \frac{1}{4}\kappa x] \sin 2\omega t \end{array} \right\} \quad (14)$$

where the expression in the curly brackets reaches a *maximum value* at the luff, where $x = 0$

$$\left\{ \frac{1}{4}(\kappa L)^2 + \frac{1}{8} \sqrt{2 - 2 \cos 2\kappa L - 4\kappa L \sin 2\kappa L + 4(\kappa L)^2 \cos(2\omega t - \phi)} \right\} \quad (15)$$

The value and distribution of the *time-averaged* tension have already been shown in the previous section; the amplitude of the *fluctuations* in tension at the luff is

$$\left(\frac{A}{L}\right)^2 m_{flag} \frac{\omega^2}{\kappa^2} \left\{ \frac{1}{8} \sqrt{2 - 2 \cos 2\kappa L - 4\kappa L \sin 2\kappa L + 4(\kappa L)^2 \cos(2\omega t - \phi)} \right\} \quad (16)$$

We can determine bounds as follows:

$$\frac{1}{4} \sqrt{(\kappa L)^2 - \kappa L} \leq \frac{1}{8} \sqrt{2 - 2 \cos 2\kappa L - 4\kappa L \sin 2\kappa L + 4(\kappa L)^2} \leq \frac{1}{4} (\kappa L + 1) \quad (17)$$

We conclude that the amplitude of the fluctuations is guaranteed to be less than the average if $L > \lambda/4$. This condition is met by typical flags, which are several wave-lengths long. When the flag is many wave-lengths long ($\kappa L \gg 1$), the fluctuations approach $\kappa L/4$, which is $1/\kappa L$ of the average value.

6 Governing Equation

Having demonstrated the importance of the dynamically-induced tension, we expand the Equation 1 to include non-linear structural terms. Using the Hamilton's Principle approach outlined by Païdoussis [17], and using the

curvilinear coordinate s along the path of the inextensible flag

$$\begin{aligned}
& m_{flag} \frac{\partial^2 w}{\partial t^2} + EI \left\{ \frac{\partial^4 w}{\partial s^4} \left[1 + \left(\frac{\partial w}{\partial s} \right)^2 \right] + 4 \frac{\partial w}{\partial s} \frac{\partial^2 w}{\partial s^2} \frac{\partial^3 w}{\partial s^3} + \left(\frac{\partial^2 w}{\partial s^2} \right)^3 \right\} \\
& - \frac{\partial^2 w}{\partial s^2} \left\{ T_{drag} \left[1 + \frac{3}{2} \left(\frac{\partial w}{\partial s} \right)^2 \right] + m_{flag} \int_s^L \int_0^s \left(\left(\frac{\partial^2 w}{\partial t \partial s} \right)^2 + \frac{\partial w}{\partial s} \frac{\partial^3 w}{\partial t^2 \partial s} \right) ds ds \right\} \\
& - \frac{\partial w}{\partial s} \left\{ \frac{\partial T_{drag}}{\partial s} \left[1 + \frac{1}{2} \left(\frac{\partial w}{\partial s} \right)^2 \right] + m_{flag} \int_0^s \left(\left(\frac{\partial^2 w}{\partial t \partial s} \right)^2 + \frac{\partial w}{\partial s} \frac{\partial^3 w}{\partial t^2 \partial s} \right) ds \right\} \\
& = \Delta p \tag{18}
\end{aligned}$$

The integral terms, generated by the in-plane component of kinetic energy, can be seen to correspond to dynamically induced tension and tension-gradient terms.

7 Conclusion

There is also a large class of practical problems in fluid-structure interaction in which dynamically induced tension is possible; examples include edge flutter in membranes, in paper webs, and in cantilevered panels. We have described the physical mechanism which is necessary to generate it; Hoerner's [18] postulation of flow separation is neither necessary nor sufficient to explain how flutter creates drag.

Induced tension is often neglected, for example by neglecting kinetic energy due to in-plane motion, when formulating the solution procedure. *Prima facie*, this appears to be justified because in-plane motion is much smaller than the out-of-plane motion. However, we have shown here the while out-of-plane motion leads to the inertia term, the in-plane motion generates integral terms that do not compete with inertia, but with skin-friction T_{drag} and stiffness EI terms. We must assess the importance of $T \partial^2 w / \partial x^2$ by comparison with $EI \partial^4 w / \partial x^4$ at the appropriate wavelength λ ; tension is negligible if

$$T \ll \left(\frac{2\pi}{\lambda} \right)^2 EI$$

The non-linear induced-tension terms, together with panel stiffness, structural nonlinearity, flow separation, *etc.*, act to limit flutter amplitudes. Flag

flutter is a good model for studying this process, because other flutter-limiting mechanisms such as plate stiffness, tension across the width (either pre-load or deflection-induced), and aerodynamic non-linearities, can all be made comparatively small, not only theoretically, but also physically. This will make it possible to isolate the dynamically-induced-tension effect, and to confirm the analysis by experimental measurements.

Acknowledgements: This work was made possible by an Alexander von Humboldt Research Award, and was carried out with suggestions and encouragement from Prof. Peter Hagedorn at T.U. Darmstadt in Germany.

References

- [1] Dieter Thoma, “Warum flattert die Fahne”, *Mitteilungen des Hydraulischen Instituts der Technischen Hochschule München*, Heft 9 (1939), pages 30–34; translation “Why does the flag flutter”, Cornell Aeronautical Laboratory, 1949.
- [2] J.A. Sparenberg, “On the waving motion of a flag”, *Proceedings Koninklijke Nederlandse Akademie van Wetenschappen*, Series B: Physical Sciences, Vol. LXV (1962), Mechanics, pages 379–392.
- [3] R.A. Fairthorne, “Drag of Flags”, *Aeronautical Research Committee (ARC) Reports and Memoranda* No. 1345 (Ae. 477), pages 887–891, Her Majesty’s Printing Office (HMSO), London 1930.
- [4] D. Thoma, “Das schlenkernde Seil” (The oscillating rope), *Z. Angew. Math. Mech. (ZAMM)*, Band 19, Nr. 5 (October 1939), pages 320–321.
- [5] Y.B. Chang, S.J. Fox, D.G. Lilley, & P.M. Moretti, “Aerodynamics of moving belts, tapes, and webs”, *ASME Machinery Dynamics and Element Vibration* DE-Vol. 36 (Sept. 1991), ASBN 0-7918-0627-8, pages 33–40; also at <http://www.mae.okstate.edu/Faculty/moretti/moretti.html>
- [6] Peter M. Moretti, *Modern Vibrations Primer*, CRC Press, Boca Raton, Florida, ©2000, ISBN 0-8493-2038-0, page 291.
- [7] Hermann Schlichting, *Boundary-Layer Theory*, translated by J. Kestin, McGraw-Hill, N.Y. 1955, Chapter VII, Section e.

- [8] *ibidem*, Chapter XXI.
- [9] S.K. Datta & W.G. Gottenberg, “Instability of an elastic strip hanging in an airstream”, *Trans. ASME, Journal of Applied Mechanics*, March 1975, pages 195–198.
- [10] Nobuyuki Yamaguchi, T. Sekiguchi, K. Yokota, & Y. Tsujimoto, “Flutter limits and behavior of a flexible thin sheet in high-speed flow—II. Experimental results and predicted behavior for low mass ratios”, *Trans. ASME, Journal of Fluids Engineering*, Vol. 122 (March 2000), pages 65–83.
- [11] Minuro Uno, “Fluttering of flexible bodies”, *Journal of the Textile Machinery Society of Japan*, Vol. 19 (1973), No. 4/5, pages 103–109.
- [12] Y. Watanabe, S. Suzuki, M. Sugihara, & Y. Sueoka, “An experimental study of paper flutter”, *Journal of Fluids and Structures*, Vol 16 (2002), No. 4, pages 529–560; see also Nobuyuki Yamaguchi, Kazuhiko Yokota, & Yoshinobu Tsujimoto, “Flutter Limits and Behaviors of a Flexible Thin Sheet in High-Speed Flow—I: Analytical Method for Prediction of the Sheet Behavior,” *Trans. ASME, J. of Fluids Engineering*, vol. 122, March 2000, pp. 65–73.
- [13] Sadatoshi Taneda, “Waving motion of flags”, *Journal of the Physical Society of Japan*, Vol 24, No. 2 (Feb. 1968), pages 392–401.
- [14] Jun Zhang, S. Childress, A. Libchaber, & M. Shelley, “Flexible filaments in a flowing soap film as a model for one-dimensional flags in a two-dimensional wind”, *Nature*, Vol. 408 (2000), pages 835–839.
- [15] D.J.J. Farnell, T. David, & D.C. Barton, “Numerical simulation of a filament in a flowing soap bubble”, correspondent Prof. David, Dept. Mech. Engrg., University of Canterbury, Christchurch, New Zealand; submitted to *International Journal for Numerical Methods in Fluids*, 2003.
- [16] <http://www.mackichan.com/>
- [17] Michael P. Païdoussis, *Fluid-Structure Interactions: Slender Structures and Axial Flow Volume 1*, Academic Press, San Diego, California, 1998, ISBN 0-12-544360-9, pages 79ff, 283f, & 502f.

- [18] Sighard F. Hoerner, *Fluid-Dynamic Drag*, publ. Hoerner Fluid Dynamics, Brick Town, N.J., 1958, section 3 - page 25.